

The role of environment on the formation of different FR type extragalactic radio sources

R. R. Andreasyan ^{*1}, G. M. Paronyan^{†1}, and A. G. Sukiasyan^{‡1}

¹NAS RA V. Ambartsumian Byurakan Astrophysical Observatory (BAO)

Abstract

We study the environment of nearby extragalactic radio sources of different morphological type from our sample. We chose 30 3C radio galaxies of different FR class for which we have several observational dates on wavelength from radio to X ray. For the study we select the regions with radius of 500 pc around of the parent galaxy of radio sources. We bring the optical maps of these regions that are overlaid on the radio maps and maps in all available wavelength. The preliminary review show that there are some differences in the neighboring regions around radio galaxies of different FR classes.

Keywords: *radio sources, FR, 3C radio galaxies*

1. Introduction.

The study of active galaxies is one of traditional direction of Byurakan observatory. In this paper we present some of our results in this direction, the study of different physical and morphological properties of extragalactic radio sources.

Extragalactic radio sources mainly are divided on two groups: compact and extended radio sources. One of the well-known classifications of extended radio galaxies is the (FR) classification of Fanaroff and Riley (Fanaroff & Riley, 1974), which is based on the radio brightness distribution over the radio image. Radio galaxies with relatively lower radio luminosity, in which the radio brightness decreases from the center to the edges, are classified as I class radio galaxies (FRI), and radio galaxies with higher radio luminosity, in which the radio brightness increases from the center to the edges of the II class (FR II). Figure 1 shows examples of extragalactic radio sources of FRI and FR II types.

At present, the Fanaroff-Riley dichotomy has been studied quite well and many other differences in physical and morphological features have been found for different classes of radio galaxies. Partly in our early studies a correlation was found between the optical and radio axes of nearby FR II radio galaxies and no correlation for FRI radio galaxies (Andreasyan & Sol, 1999) (Fig.2 left); a correlation of the average radio polarization angles with the radio axes for nearby FR II radio galaxies and no correlation for FRI radio galaxies (Andreasyan et al., 2002) (Fig.2 right); a correlation of the ellipticity of parent optical galaxies associated with radio galaxies of different classes (Andreasyan & Sol, 2000) (Fig 3), etc. For the study we use data of nearby extragalactic radio sources from our samples (Andreasyan & Abrahamyan, 2021). In these samples we have data for 267 nearby radio galaxies identified with elliptical galaxies brighter than 18th magnitude (sample1) and 280 extragalactic radio sources with known position angles between the integrated intrinsic radio polarization and radio axes (sample 2). For these radio galaxies we bring the following data: Radio Sours Name, oPA - the position angle of the major axis of optical galaxy, rPA - the position angle of radio axis, dPA - the relative position angle between optical and radio axes, E - the ellipticity of the optical galaxy identified with radio sources, FR - the Fanaroff Riley class, M - the optical magnitude, SI - the spectral index, z - the redshift, logP - the radio luminosity, K - the ratio of major to minor axis of radio image, Ref. for the radio maps and FR classes.

Here are some results from our above-mentioned papers.

*randreasyan@gmail.com, Corresponding author

†paronyan_gurgen@yahoo.com

‡andranik.suqiasyan.1995@mail.ru

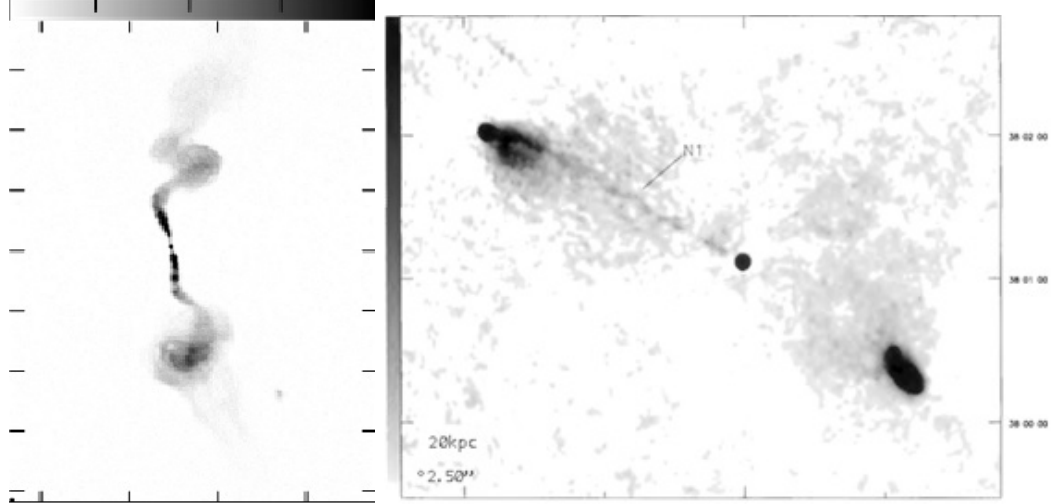


Figure 1. Extragalactic radio sources of FRI type 3C449 (left) and FR II type 3C111 (right).

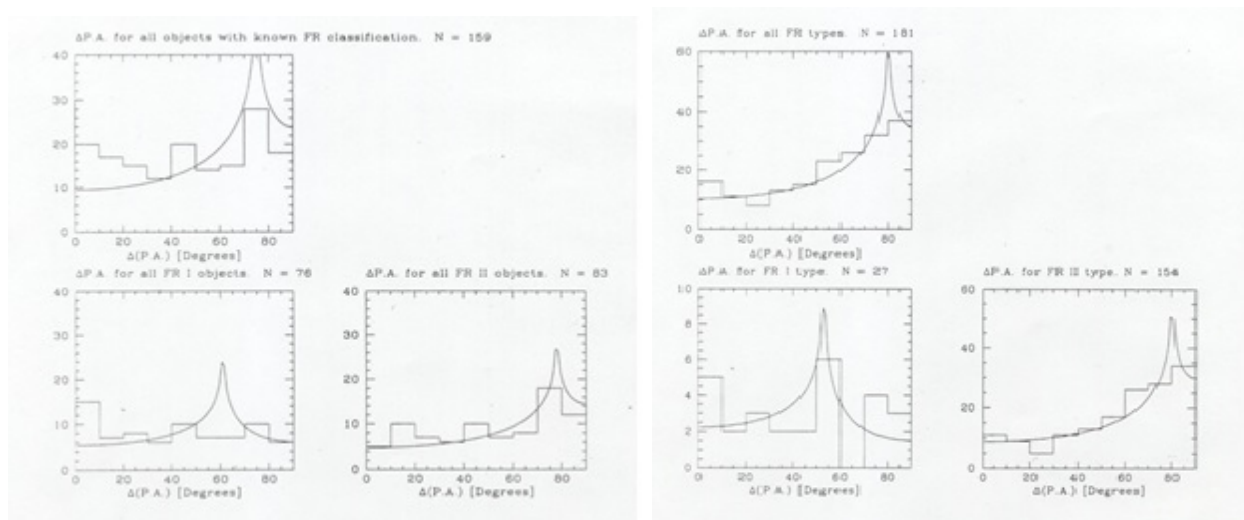


Figure 2. The distribution of angles between the optical and radio axes (left) and angles between average radio polarization and radio axes (right).

The ellipticity of parent optical galaxies of FR II type radio galaxies is larger than the ellipticity of parent optical galaxies of FRI type objects.

These large differences in morphology and physical properties of different classes of extragalactic radio sources can be due to differences in parent optical galaxies or in differences of the extragalactic medium around the radio source in which the radio source is expanding.

In order to reveal the influence of the environment on extragalactic radio source, we study the close proximity (regions with radius of 500 pc around of the central radio galaxies) of the well-known Giant radio sources 3C31, 3C449, NGC315, NGC6251 from our sample of about 30 nearby 3C radio galaxies of different FR types chosen from (Andreasyan & Abrahamyan, 2021).

2. The study of the neighborhood of radio galaxies.

For the study we construct the maps of optical galaxies that are overlaid on the radio map of 3C radio source. We use also the maps of these regions in all available wavelength. Here we present more detail analyses and new results for the radio galaxy of FRI type 3C31.

The 3C 31 class FRI radio source has been identified with the NGC 383 parent galaxy, which is the central object of the group of galaxies, which in turn is a member of the Perseus-Pisces supercluster (Sakai et al., 1994) and has been studied quite well. Numerous results and useful data have now been obtained

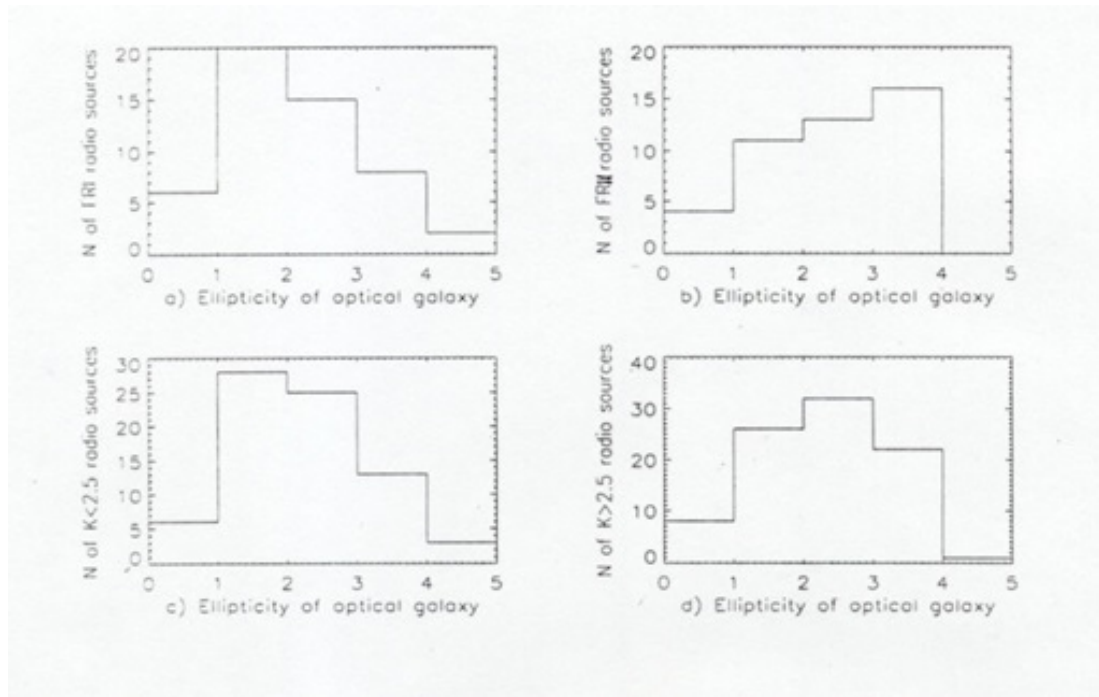


Figure 3. The ellipticity of optical parent galaxies for different FR types and for different classes of K classification.

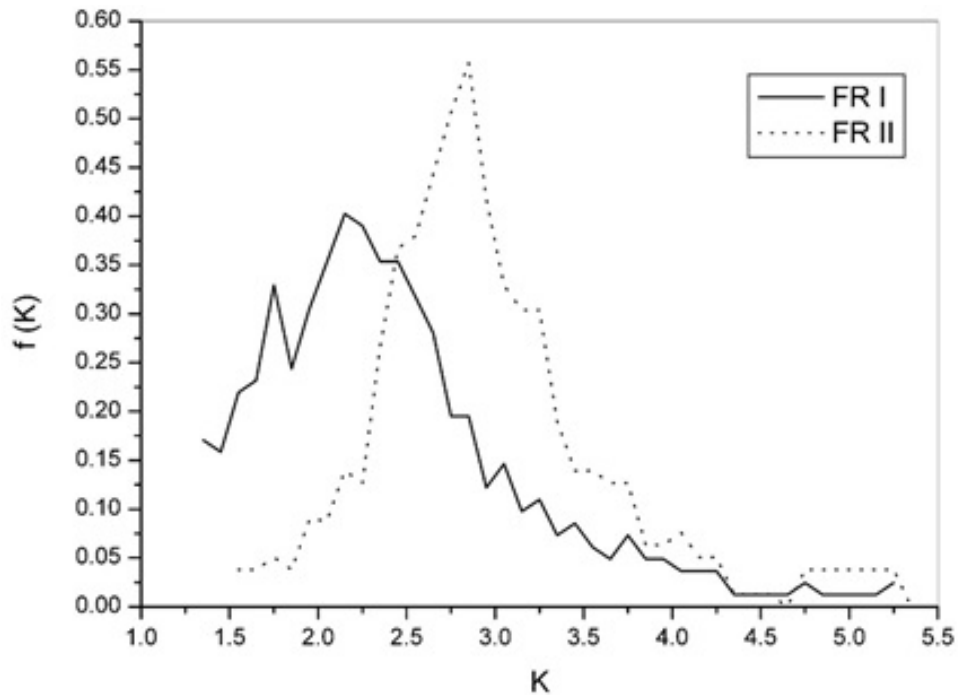


Figure 4. The distribution function from elongation parameter K for FRI and FRII class radio galaxies.

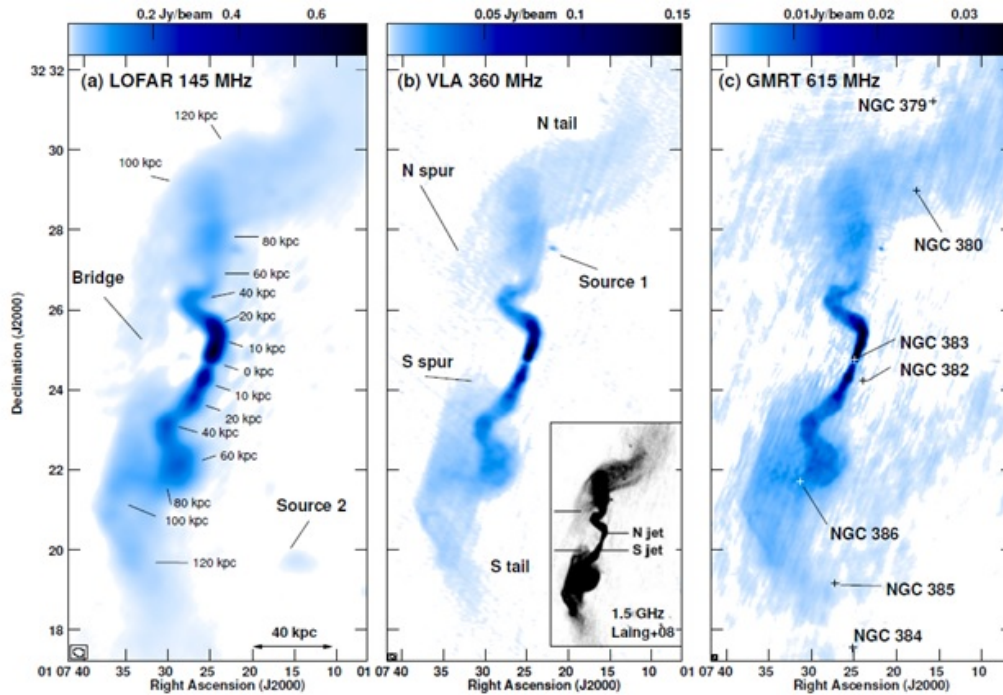


Figure 5. Radio image maps of the FRI class radio galaxy 3C 31 at three different frequencies (Heesen et al., 2018)

for these objects (Croston & Hardcastle, 2014, Hardcastle et al., 2002, Laing & Bridle, 2002, Martel et al., 1999, Parma et al., 1999, Strom et al., 1983). Of these, here we highlight some of the data of interest to us, which can be used in the present work. On figure 5 we bring the radio map of 3C31 at frequency of 1400 MHz (corresponding to FIRST observations) with the overlaid optical region with the central galaxy NGC 383. As it is seen a group of galaxies in the form of a chain has the direction of the radio image. It is more obvious on the figure 6 of same region from the paper (Heesen et al., 2018) at different frequencies, 145, 360 and 615 MHz corresponding to LOFAR, VLA and GMRT observations, respectively.

From figures we see that the elliptical galaxies NGC 380 and NGC 386 are located respectively in the northern and southern parts of the 3C31 radio image. These galaxies, together with the central SA0 type galaxy of the group NGC 383 are on the same line, the direction of which coincides with the direction of central part of radio image with great accuracy.

Radio jet simulations (Laing & Bridle, 2002) have shown that the direction of the central jet is approximately 52° with the line of sight. Moreover, the northern part of the jet approaches the observer, while the southern part moves away. On the other hand, the analysis of the redshifts of the mentioned optical galaxies shows that the relative line of sight velocity of the northern galaxy NGC 380 compared to the central galaxy NGC 383 is directed towards the observer as for the northern jet, and the relative velocity of the southern galaxy NGC 386 is directed away from the observer as for the southern jet. This probably suggests that the direction of the spatial velocities of these galaxies also coincides with the direction of the velocities of the radio jets and, therefore, galaxies NGC 380 and NGC 386 move away from the central galaxy NGC 383 in opposite directions coincide with the direction of the radio jets.

We calculated the time of removal of galaxies from the central galaxy. The calculation results are shown in Table 1. Δz is difference of redshifts from the central galaxy NGC 383, ΔV and ΔV_0 – the relative line of sight and spatial velocities respectively, d and d_0 – the projected on the sky and spatial distances, T – the time of removal of galaxies.

Table 1. Results of Calculations.

Galaxies	Δz	ΔV	ΔV_0	d	d_0	T
NGC380	-0.00224	-672	1092	97.07	123.2	110
NGC386	+0.00153	+459	745.5	70.64	89.64	118

The table shows that the galaxies NGC 380 and NGC 386 were near the galaxy NGC 383 about 110

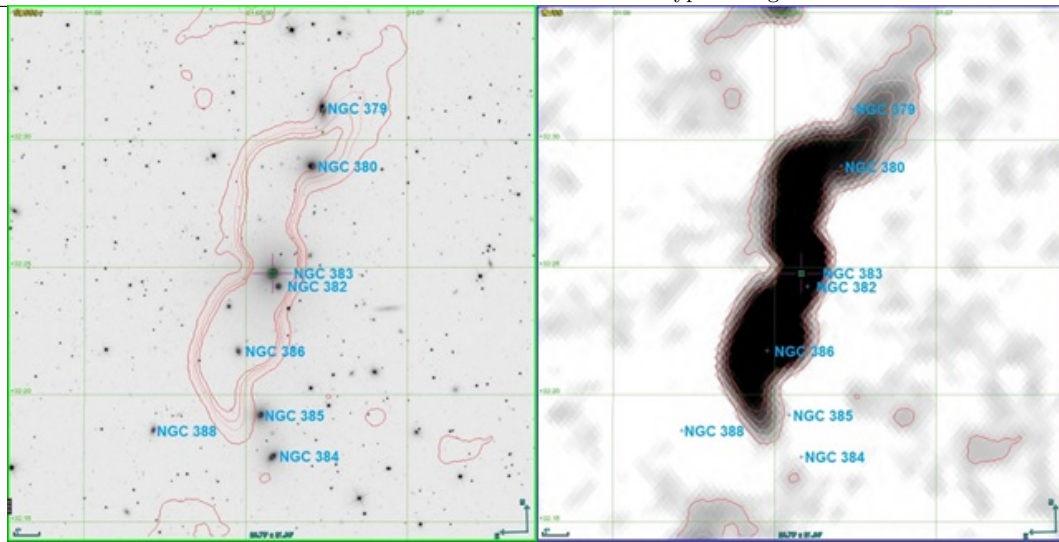


Figure 6. The region of a group of galaxies with the central object NGC 383 and radio source 3C31 of the FRI class at a frequency of 1400 MHz.

million years ago. A very close passage of these three galaxies then probably occurred, after which the recession of the galaxies NGC 380 and NGC 386 from the more massive central galaxy NGC383 began. A natural question arises whether such a close passage can be the cause (trigger) of the beginning of radioactivity of the central galaxy. As a reliable argument for such assumption can be the result of the modeling of the spectral characteristics of the radio emission of the central part of the radio galaxy 3C31 that gives an estimate of the age of the central jet of about 100 million years (Heesen et al., 2018).

References

- Andreasyan R. R., Abrahamyan H. V., 2021, *Communications of the Byurakan Astrophysical Observatory*, 68, 75
- Andreasyan R. R., Sol H., 1999, *Astrophysics*, 42, 275
- Andreasyan R. R., Sol H., 2000, *Astrophysics*, 43, 413
- Andreasyan R. R., Appl S., Sol H., 2002, *Astrophysics*, 45, 198
- Croston J. H., Hardcastle M. J., 2014, *Mon. Not. R. Astron. Soc.* , 438, 3310
- Fanaroff B. L., Riley J. M., 1974, *Mon. Not. R. Astron. Soc.* , 167, 31P
- Hardcastle M. J., Worrall D. M., Birkinshaw M., Laing R. A., Bridle A. H., 2002, *Mon. Not. R. Astron. Soc.* , 334, 182
- Heesen V., et al., 2018, *Mon. Not. R. Astron. Soc.* , 474, 5049
- Laing R. A., Bridle A. H., 2002, *Mon. Not. R. Astron. Soc.* , 336, 328
- Martel A. R., et al., 1999, *Astrophys. J. Suppl. Ser.* , 122, 81
- Parma P., Murgia M., Morganti R., Capetti A., de Ruiter H. R., Fanti R., 1999, *Astron. Astrophys.* , 344, 7
- Sakai S., Giovanelli R., Wegner G., 1994, *Astron. J.* , 108, 33
- Strom R. G., Fanti R., Parma P., Ekers R. D., 1983, *Astron. Astrophys.* , 122, 305